JACS
JOURNAL OF THE AMERICAN CHEMICAL SOCIETY
Article
pubs.acs.org/JACS

Iterative Reductive Aromatization/Ring-Closing Metathesis Strategy toward the Synthesis of Strained Aromatic Belts

Matthew R. Golder,[†] Curtis E. Colwell,[†] Bryan M. Wong,[‡] Lev N. Zakharov,[§] Jingxin Zhen,[∥] and Ramesh Jasti*[,†]

[†]Department of Chemistry & Biochemistry and Material Science Institute, University of Oregon, Eugene, Oregon 97403, United States

[‡]Department of Chemical & Environmental Engineering and Materials Science & Engineering Program, University of California—Riverside, Riverside, California 92521, United States

[§]CAMCOR − Center for Advanced Materials Characterization in Oregon, University of Oregon, Eugene, Oregon 97403, United States

[∥]Department of Chemistry, Boston University, Boston, Massachusetts 02215, United States

Supporting Information

ABSTRACT: The construction of all sp^2-hybridized molecular belts has been an ongoing challenge in the chemistry community for decades. Despite numerous attempts, these double-stranded macrocycles remain outstanding synthetic challenges. Prior approaches have relied on late-state oxidations and/or acid-catalyzed processes that have been incapable of accessing the envisaged targets. Herein, we describe the development of an iterative reductive aromatization/ring-closing metathesis approach. Successful syntheses of nanohoop targets containing benzo[*k*]tetraphene and dibenzo[*c*,*m*]-pentaphene moieties not only provide proof of principle that aromatic belts can be derived by this new strategy but also represent some of the largest aromatic belt fragments reported to date.

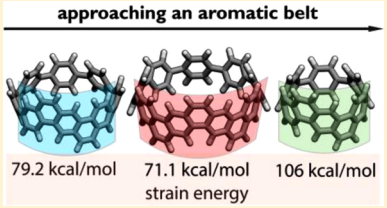

INTRODUCTION

Double-stranded macrocyclic targets containing solely sp^2-hybridized carbons, colloquially known as "aromatic belts", have evaded synthesis by organic chemists for decades.[1] These molecules are prized for their severely distorted and strained aromatic systems with unique inwardly facing π-systems. As defined by Scott, true graphitic belts are "distinguished by the presence of upper and lower edges that are conjugated but never coincide."[2] These compounds have also been identified as short sections of carbon nanotubes, further heightening the interest in the synthesis of these types of structures. In 1987, Stoddart was able to access late-stage intermediate kohnkene[3] en route to $[6]_{12}$cyclacene, but was plagued by the final oxidation step (Figure 1a). Presumably, the harsh oxidative conditions were either incompatible with the product or incapable of building the required amount of strain.[3,4] Herges surmised that a picotube precursor could afford [4]-cyclophenacene, but oxidative and flash vacuum pyrolysis (FVP) conditions only led to polymeric and rearranged products, respectively (Figure 1b).[5] Cory, Schlüter, Iyoda, and Vollhardt have also made contributions toward the syntheses of [*n*]cyclacenes and [*n*]cyclophenacenes, but their efforts were again thwarted by harsh, late-stage reaction conditions.[6] Most recently, the Scholl reaction,[7] widely used in the syntheses of a myriad of polycyclic aromatic hydrocarbons (PAHs),[8] has appeared to be a promising approach to access aromatic belts from arylated [*n*]CPPs *a priori*, but as recently shown by the Müllen group[9] and our group,[10] the conditions are typically incompatible with [*n*]cyclopara-phenylene backbones due to the propensity for strain-relieving 1,2-aryl shifts. While the bottom-up syntheses of these challenging macrocycles have been unsuccessful thus far, elegant work from the Nakamura group[11] has allowed access to an electronically isolated fullerene-derived [10]-

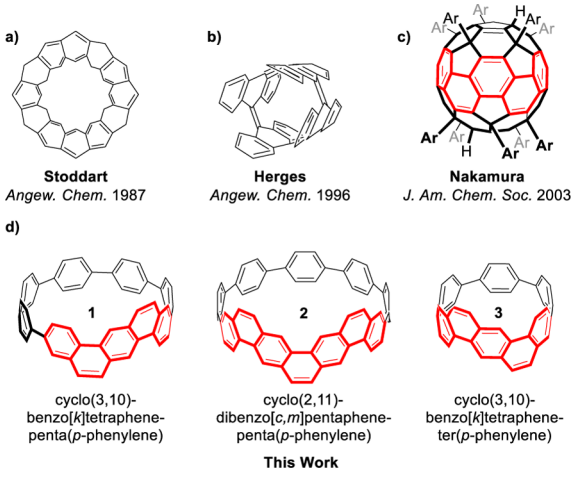

Figure 1. Representative work on aromatic belts (a−c) and aromatic belt fragments **1**, **2**, and **3**.

Received: March 5, 2016
Published: April 30, 2016

DOI: 10.1021/jacs.6b02240
J. Am. Chem. Soc. 2016, 138, 6577−6582

cyclophenacene through systematic, top-down degradation of C_{60} (Figure 1c).

With the need for new strategies to access these strained belt structures, we hypothesized that an approach leveraging both reductive aromatization and ring-closing metathesis methodologies could allow access to this family of aromatic belts. In addition to work on the synthesis of [*n*]cycloparaphenylenes coming from Itami, Yamago, and others,[12] our laboratory has demonstrated the power of oxidative dearomatization/reductive aromatization strategies toward highly strained, all sp^2-hybridized nanohoops.[13] Additionally, PAHs[14] such as sumanene,[15] septulene,[16] and [*n*]helicenes[17] have been accessed via ring-closing metathesis (RCM)—a mild, redox-neutral process, although such molecules do not present the same challenges offered by these belt structures. We envisioned merging these two processes in an approach that could ultimately lead to aromatic belts. Herein, we report the development of an iterative reductive aromatization/ring-closing metathesis strategy to synthesize aromatic belt fragments **1**, **2**, and **3**. These studies not only validate the general approach but also provide some of the largest all sp^2-hybridized belt fragments prepared to date.

RESULTS AND DISCUSSION

Synthesis and Characterization. Schemes 1 and 2 illustrate our first-generation approach to this class of molecules. Synthesis of **1** and **2** commenced with the twofold lithiation of *syn*-dibromide **4**, followed by addition of 2 equiv of benzoquinone monoketal (Scheme 1). Following deprotection, diquinol **5** was accessed in 44% yield. We have previously shown that additions of aryl lithium reagents to *p*-quinols in the presence of sodium hydride preferentially affords the syn diastereomer (dr >19:1) as dictated by an electrostatic model.[13b] Hence, lithiation of **6a** followed by twofold diastereoselective addition to **5** and *in situ* methylation of the resulting tetra-alkoxide allowed for rapid formation of dichloride **7** in 36% yield (dr = 9:1, syn−syn/syn−anti).

Scheme 1. Synthesis of Dichloride 8

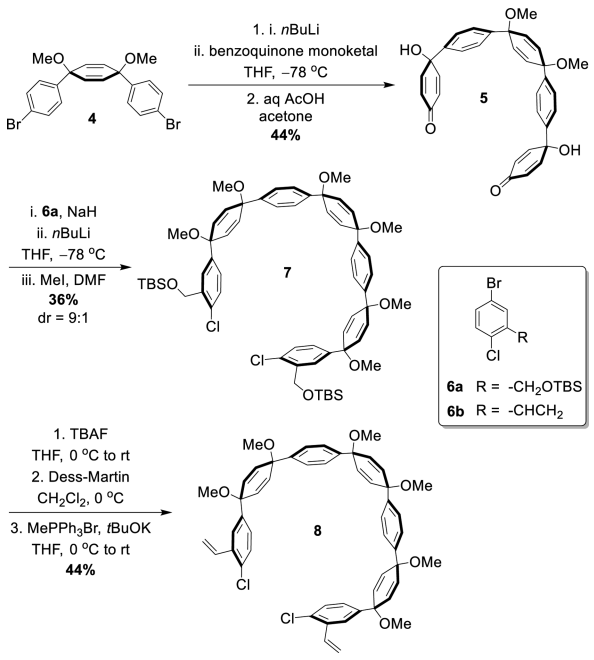

Scheme 2. Synthesis of Vinylated Macrocycles 10 and 12

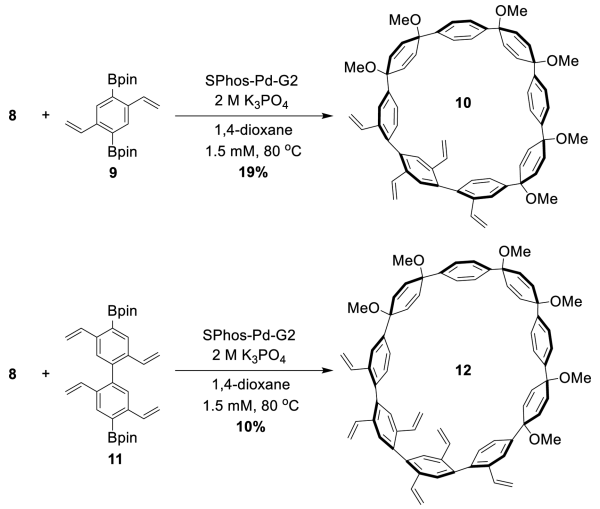

Deprotection with TBAF, followed by oxidation with Dess-Martin periodinane and Wittig olefination, afforded dichloride **8** in 44% yield over three steps. Attempts to directly access divinyl **8** from precursor **6b** were unsuccessful due to undesirable anionic polymerization of the styrene moiety.

Having accessed precursor **8**, we were in position to explore macrocyclization reactions.[13c,d] In previous work, we had yet to explore the generation of macrocycles where both coupling partners possessed ortho functionality.[18] Initial treatment of fragments **8** and **9** with 20 mol % SPhos-Pd-G2[19] in dioxane/water (9:1, ca. 1.5 mM) at 80 °C afforded terphenyl-containing macrocycle **10** in 19% yield (Scheme 2). To access an even more elaborate system, the use of biphenyl diboronic acid (bis)pinacolester **11** as a coupling partner afforded macrocycle **12** in 10% yield. Interestingly, macrocycles **10** and **12** display different dynamic properties as evidenced by VT-NMR spectroscopy. Based on the sharp proton resonances of **10** and the broadened signals for **12**, we can conclude that compound **10** adopts a single low-lying conformation while **12** exists as a series of slowly interconverting conformers at room temperature (Figures S15−S16). Upon heating to 70 °C, the ^{1}H NMR signals of **12** sharpen, whereas the signals for **10** broaden. Presumably, at elevated temperatures, **12** can rapidly interconvert between conformers whereas **10** is slowly interconverting between a series of energetically similar conformations. A computational analysis of the various atropisomers that **10** and **12** can adopt is consistent with these NMR experiments (Tables S4−S5).

With macrocycles **10** and **12** in hand, we next tested the key RCM and reductive aromatization reactions. Since the reductive aromatization of these systems typically requires strong reductants such as sodium naphthalenide, which we anticipated to be problematic in the context of the styrene functionality, we opted to investigate the RCM reaction first. Macrocycles **10** and **12** were each subjected to Grubbs' second generation catalyst (Grubbs II) in dichloromethane at 40 °C (Scheme 3).[14] Gratifyingly, **10** and **12** were cleanly converted to **13** and **14**, respectively, without any evidence of cyclohexadiene degradation. Not surprisingly, the terminal olefins react significantly faster than the disubstituted cyclohexadiene olefins; in fact, the reaction time can be prolonged to 5 h without any observable byproducts or decrease in yield. Subjecting **13** to sodium naphthalenide at −78 °C afforded

DOI: 10.1021/jacs.6b02240
J. Am. Chem. Soc. 2016, 138, 6577−6582

Scheme 3. Ring-Closing Metathesis/Reductive Aromatization Sequence towards 1 and 2

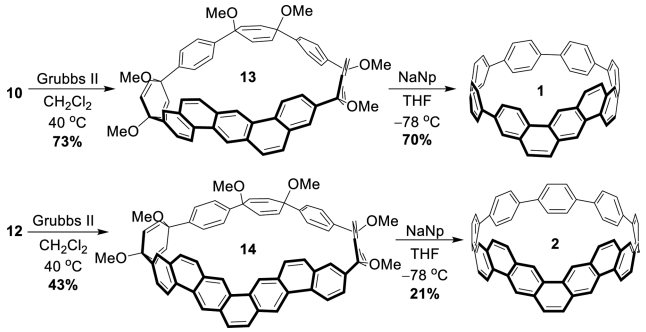

cyclo(3,10)-benzo[*k*]tetraphene-penta(*p*-phenylene) **1** in 47% yield (Scheme 3). Reductive aromatization of **14** at −78 °C delivered cyclo(2,11)-dibenzo[*c*,*m*]pentaphene-penta(*p*-phenylene) **2** in 21% yield. Insofar as we know, a dibenzo[*c*,*m*]-pentaphene moiety was synthesized for just the second time in accessing **2**.[20] Advantageously, incorporation of dibenzo[*c*,*m*]-pentaphene into a macrocycle increases solubility relative to the completely insoluble acyclic PAH counterpart reported by Clar. Furthermore, while several large PAH units have been incorporated into various cyclophanes,[12c,21] **1** and **2** represent some of the largest PAHs to be incorporated into an all sp^2-hybridized backbone thus far.[22]

Although the syntheses of structures **1** and **2** validated the basic RCM/reductive aromatization approach, our initial studies also revealed several key issues. First, the use of protected alcohols as vinyl surrogates is a cumbersome approach to the requisite alkenes. Furthermore, when the synthesis of [*n*]cyclophenacenes was preemptively considered, it was noted that functionalization will be required on the cyclohexadiene rings, leading to macrocyclic intermediates possessing multiple stereocenters. In these cases, it would be much more desirable to *execute the reductive aromatization prior to RCM*, thereby eliminating potential issues of mismatched chirality between functionalized cyclohexadiene rings during the metathesis events. In addition to these points, we were also curious if smaller, more highly strained belts could be accessed through a combination of reductive aromatization and ring-closing metathesis methodology. A new target (**3**) was chosen to investigate a revised second-generation methodology that would address these challenges. First, simple allyl groups were incorporated to TES-protected quinol **15** as vinyl surrogates for the RCM reaction (Scheme 4). Monolithiation of *p*-dibromobenzene followed by subsequent addition of ketone **15** yields an aryl bromide that can undergo a second lithiation followed by addition to ketone **15** again to rapidly provide a five-ring macrocycle precursor in one pot isolated as a single diastereomer. The crude diol can then be protected using triethysilyl chloride, followed by base catalyzed olefin isomerization to yield precursor **16** in 38% yield over three steps. Dichloride **16** and bisboronate **9** undergo Suzuki coupling under standard conditions to deliver macrocycle **17** in 11% yield. The subsequent silyl deprotection followed by reductive aromatization under mild conditions recently reported by Yamago[23] yields **18**, with no evidence of styrene decomposition. Ring-closing metathesis then afforded cyclo(3,10)-benzo[*k*]tetraphene-ter(*p*-phenylene) **3** in an unoptimized 17% yield. This second-generation approach, in which the reductive aromatization can be carried out prior to the RCM reaction,

Scheme 4. Second Generation Approach to Cyclo(3,10)-benzo[*k*]tetraphene-ter(*p*-phenylene) 3

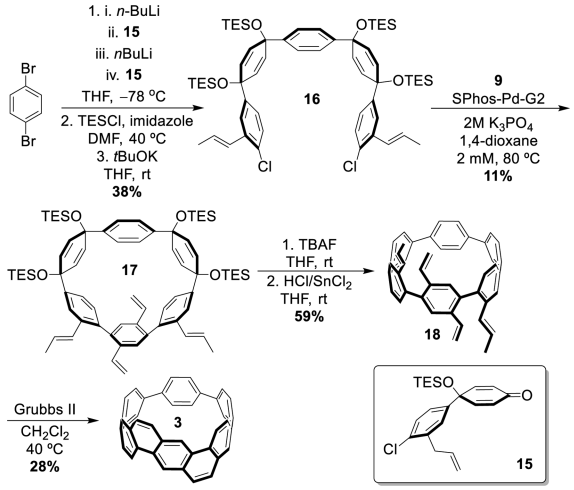

provides a concise synthesis of the most strained of the three belt fragment targets accessed. Furthermore, the synthesis of **18** addresses a longstanding problem with the functionalization of [*n*]cycloparaphenylenes by offering four substituents along the backbone with precise regiochemistry.[24]

Solid State Analysis. The solid-state structures of the two aromatic belt fragments **1** and **2** were evaluated through X-ray crystallographic analysis.[25] Molecule **1** crystallized as a racemate, and the benzo[*k*]tetraphene group was disordered over at least four different positions (Figure S1). Hence, we were unable to glean any detailed structural data from the crystal structure of **1**. On the other hand, crystallization of achiral **2** proved to be more successful, leading to two symmetrically independent molecules in the asymmetric unit (Figure S2). The nanohoops form "head-to-tail" pairs with the PAH motif of one nanohoop in alignment with the polyphenylene backbone of a second nanohoop. Through an analysis of the solid-state structure of **1**, we also determined that the incorporation of a large PAH led to some structural differences compared to [9]CPP.[26] Although the average C_{ipso}−C_{ipso} bond length between nonfused phenyl rings in **1** was identical to that of [9]CPP (1.47 Å), the average torsional angle between the same rings increased from 24.4° in [9]CPP to 31.5° in **1** (Table S1). Moreover, based on the parameters defined by Bodwell and co-workers, we determined that the total bend (θ)[27] of the fully conjugated dibenzo[*c*,*m*]-pentaphene unit was 134°, 33° less bent than Bodwell's alkyl-bridged [8](2,11)teropyreneophane (θ = 167°).[28] We were unable to obtain a crystal structure of compound **3**, but we evaluated the total bend as 142° based on a DFT optimized structure (Figure 2).

Optical and Electrochemical Analysis. We next characterized the optical and electrochemical properties of all three new structures.[29] To begin, we acquired UV−vis spectra for **1**−**3** and compared the results to data from the three parent [*n*]CPPs ([8]-, [9]-, and [6]CPP, respectively) (Figure 3). While [*n*]CPPs always have a major absorption centered around 340 nm arising from a number of degenerate orbital transitions,[30] the major absorptions for **1**−**3** are, in order of increasing nanohoop diameter, 310 nm (**3**), 325 nm (**1**), and 340 nm (**2**). As the size of the nanohoop decreases (**2** → **1** → **3**), more fine structure in the spectra become apparent. We surmise that the increased rigidity of the smaller structures is

DOI: 10.1021/jacs.6b02240
J. Am. Chem. Soc. 2016, 138, 6577−6582

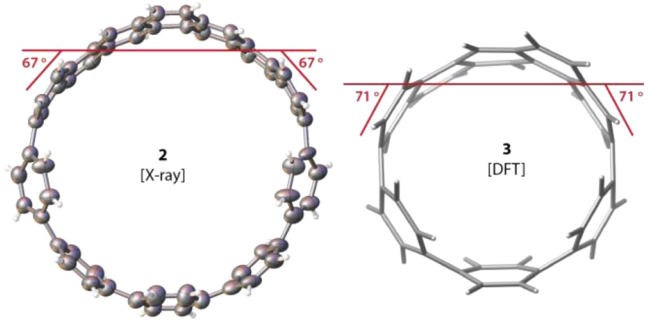

Figure 2. Comparison of total bend (θ) of dibenzo[*c*,*m*]pentaphene unit of **2** and benzo[*k*]tetraphene unit of **3**. Thermal ellipsoids (**2**) are shown at 30% probability. DFT optimization (**3**) was performed at the B3LYP-6-31G(d) level of theory. θ is defined as the sum of the indicated exterior angles.

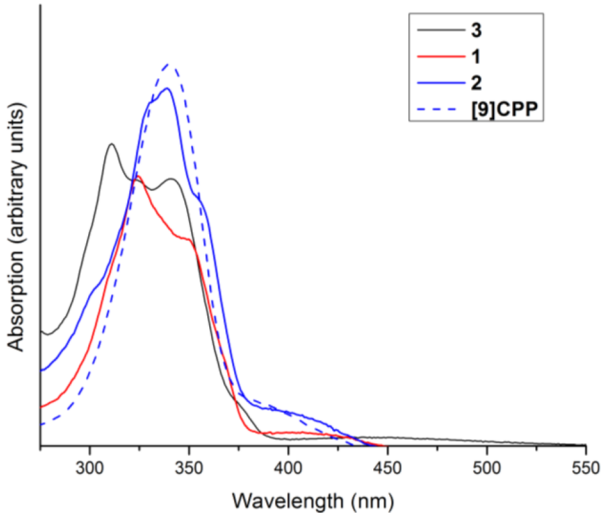

Figure 3. UV−vis spectra of **1**−**3** and [9]CPP. Absorption intensities have been adjusted to display all features on the same scale. For more details on photophysical measurements, please see Figures S3, S4, and S8 in the Supporting Information.

responsible for the observation of the most additional features in **3**. In the case of the [*n*]CPPs, absorbances corresponding to the HOMO−LUMO transition are either completely absent or very weak due to the centrosymmetric nature of the molecules.[30b,31] These minor absorbances red-shift with decreasing CPP size, a trend that is exactly opposite to that of linear oligophenylenes and a unique feature of the nanohoop structures.[13,31c] Similarly, in the case of **1**−**3**, the absorption band corresponding to the HOMO−LUMO transition is also very weak but red-shifts with decreasing hoop size, 409 nm for **2**, 417 nm for **1**, and 450 nm for **3**. For **2** and **1**, the HOMO−LUMO transitions are slightly red-shifted compared to those of [9]CPP (399 nm) and [8]CPP (409 nm), while the HOMO−LUMO transition of **3** is roughly the same as that of [6]CPP (450 nm). A first approximation based on solid-state analyses of **2** and [9]CPP suggest that the observed red-shifted HOMO−LUMO transitions could arise from the slight decrease in the average dihedral angle upon PAH incorporation into the *p*-phenylene backbone (Table S1). Further investigations of the HOMO and LUMO levels by electrochemistry and DFT computations were consistent with our UV−vis measurements (Table 1). For example, cyclic voltammetry (CV) revealed very similar cathodic half-wave potentials between **1**−**3** and their respective parent CPPs.[32] This is also consistent with the similarities observed in the calculated HOMO levels and the uniform orbital density observed for all of the HOMOs (Figures S5−S7). The LUMO energies, however, are slightly stabilized for **1**−**3** compared to [8]-, [9]-, and [6]CPP. Overall, the computed HOMO−LUMO gaps for **1**−**3** are slightly lower than the [*n*]CPP series, which is consistent with the red-shifted minor absorptions observed for **1** and **2** compared to [8]- and [9]CPP, respectively. The minor UV−vis absorption for **3** may also be red-shifted compared to the analogous transition for [6]CPP, but the weak, broad nature of these two features make it difficult to compare their absolute maxima.

Strain Energy Analysis. Finally, we evaluated the strain energies of **1**−**3**, as well as the strain energy of the corresponding precursors, computationally using homodesmotic reactions using Gaussian09[33] at the ωB97D /6-31G(d) level of theory (Scheme 5). We first determined that **1** has 79.2

Scheme 5. Evaluation of the Origins of Strain Energy in 1− 3

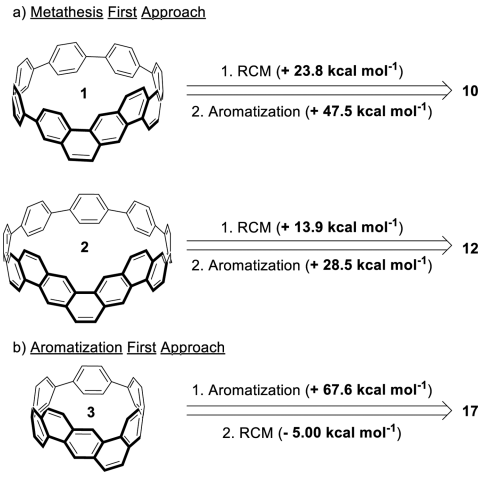

Table 1. Selected Electrochemical and Computational Data for 1−3 and Parent [*n*]CPPs

	HOMO−LUMO absorption (nm)	experimental oxidation potential (V vs Fc/Fc^+)	calculated HOMO−LUMO gap (eV)[d]
[6]CPP	450	0.44[a]	3.14[c]
3	450	0.40[b]	2.96
[8]CPP	409	0.59[c]	3.41[c]
1	417	0.60[b]	3.26
[9]CPP	399	0.70[c]	3.41[c]
2	409	0.75[b]	3.32

[a]Reference 12 (solvent = CH_2Cl_2). [b]**1** and **2** were measured in CH_2Cl_2; **3** was measured in THF. [c]Reference 31d (solvent = $C_2H_2Cl_4$). [d]Calculated at the B3LYP/6-31G(d) level of theory.

DOI: 10.1021/jacs.6b02240
J. Am. Chem. Soc. 2016, 138, 6577−6582

kcal mol^{-1} of strain energy (Scheme S3), while **2** has 71.1 kcal mol^{-1} of strain energy (Scheme S6) relative to acyclic counterparts. The smallest of our belt fragments, **3**, has a strain energy of 106 kcal mol^{-1}. Interestingly, these values are only 5−9 kcal mol^{-1} higher than their parent [8]-, [9]-, and [6]CPP analogues which have 72, 66, and 97 kcal mol^{-1} of strain energy, respectively.[13f,34] Evaluation of penultimate macrocycles **13** and **14** indicates that the powerful reductive aromatization step builds in 47.5 kcal mol^{-1} of strain (31.5 kcal mol^{-1} → 79 kcal mol^{-1}) and 28.5 kcal mol^{-1} of strain (42.6 kcal mol^{-1} → 71.1 kcal mol^{-1}) in the formation of **1** and **2**, respectively (Schemes S2 and S5). More importantly, however, RCM is able to build in 23.8 kcal mol^{-1} (7.75 kcal mol^{-1} → 31.5 kcal mol^{-1}) and 13.9 kcal mol^{-1} (28.7 kcal mol^{-1} → 42.6 kcal mol^{-1}) of strain energy during the transformations of **10** → **13** and **12** → **14**, respectively (Schemes S1 and S4). Hence, in these cases, ring-closing metathesis acts in conjunction with the Suzuki−Miyaura macrocyclization and sodium naphthalenide promoted reductive aromatization to allow for a gradual increase in strain energy. We next evaluated the energy landscape of our second-generation approach. Interestingly, in this case, the ring-closing metathesis event is a strain relieving process rather than a strain building process. Upon building in 43.4 kcal mol^{-1} during the macrocyclization step in the synthesis of **17** (Scheme S7), reductive aromatization afforded **18**, a molecule with almost as much strain energy as [5]CPP (111 kcal mol^{-1} versus 119 kcal mol^{-1}) (Scheme S8). We attribute the high strain energy of **18** to unfavorable steric interactions between *ortho*−*ortho* groups forced into close proximity with one another due to the rigid geometry of such a small macrocycle. Finally, reductive aromatization of **18** afforded **3**, which is 5 kcal mol^{-1} less strained than its penultimate intermediate (111 kcal mol^{-1} → 106 kcal mol^{-1}) (Scheme S9). We anticipate that this second-generation approach will prove to be promising methodology toward the synthesis of members in the [*n*]cyclophenacene family.

CONCLUSION

In conclusion, we have developed a reductive aromatization/ring-closing metathesis sequence for the synthesis of aromatic belt fragments. Most significantly, we have demonstrated that the RCM reaction can be carried out on highly strained systems without intervening acid-catalyzed rearrangements or undesirable oxidative processes that have plagued previous synthetic approaches. In addition, we also report an allyl isomerization strategy as an efficient method to introduce sensitive styrenyl functionality required for the RCM reactions. Our campaign toward the total synthesis of several elusive [*n*]cyclophenacene targets is well underway in our laboratory and will be reported in due course.

ASSOCIATED CONTENT

Supporting Information

The Supporting Information is available free of charge on the ACS Publications website at DOI: 10.1021/jacs.6b02240.

Crystallographic data for **1** (CIF)

Crystallographic data for **2** (CIF)

General synthetic details, NMR spectra, computational details, optical spectra, and electrochemical characterization (PDF)

AUTHOR INFORMATION

Corresponding Author

*E-mail: rjasti@uoregon.edu.

Notes

The authors declare no competing financial interest.

ACKNOWLEDGMENTS

Financial support was provided by the National Science Foundation (CHE-1255219), the Sloan Foundation, the Camille and Henry Dreyfus Foundation, and generous startup funds from the University of Oregon. M.R.G. thanks Vertex Pharmaceuticals for a graduate research fellowship. HRMS data were obtained at the Biomolecular Mass Spectrometry Core of the Environmental Health Sciences Core Center at Oregon State University (NIH P30ES000210). Mr. Evan Darzi is acknowledged for the synthesis of **5**.

REFERENCES

(1) (a) Schröder, A.; Mekelburger, H.-B.; Vögtle, F. *Top. Curr. Chem.* **1994**, *172*, 179. (b) Tahara, K.; Tobe, Y. *Chem. Rev.* **2006**, *106*, 5274. (c) Eisenberg, D.; Shenhar, R.; Rabinovitz, M. *Chem. Soc. Rev.* **2010**, *39*, 2879. (d) Evans, P. J.; Jasti, R. *Top. Curr. Chem.* **2012**, *349*, 249.

(2) Scott, L. T. *Angew. Chem., Int. Ed.* **2003**, *42*, 4133.

(3) Kohnke, F. H.; Slawin, A. M. Z.; Stoddart, J. F.; Williams, D. J. *Angew. Chem., Int. Ed. Engl.* **1987**, *26*, 892.

(4) (a) Ashton, P. R.; Isaacs, N. S.; Kohnke, F. H.; Slawin, A. M. Z.; Spencer, C. M.; Stoddart, J. F.; Williams, D. J. *Angew. Chem., Int. Ed. Engl.* **1988**, *27*, 966. (b) Ashton, P. R.; Brown, G. R.; Isaacs, N. S.; Giuffrida, D.; Kohnke, F. H.; Mathias, J. P.; Slawin, A. M. Z.; Smith, D. R.; Stoddart, J. F.; Williams, D. J. *J. Am. Chem. Soc.* **1992**, *114*, 6330. (c) Girreser, U.; Giuffrida, D.; Kohnke, F. H.; Mathias, J. P.; Philp, D.; Stoddart, J. F. *Pure Appl. Chem.* **1993**, *65*, 119.

(5) (a) Kammermeier, S.; Jones, P. G.; Herges, R. *Angew. Chem., Int. Ed. Engl.* **1996**, *35*, 2669. (b) Kammermeier, S.; Herges, R. *Angew. Chem., Int. Ed. Engl.* **1996**, *35*, 417. (c) Kammermeier, S.; Jones, P. G.; Herges, R. *Angew. Chem., Int. Ed. Engl.* **1997**, *36*, 2200. (d) Deichmann, M.; Näther, C.; Herges, R. *Org. Lett.* **2003**, *5*, 1269.

(6) (a) Cory, R. M.; McPhail, C. L. *Tetrahedron Lett.* **1996**, *37*, 1987. (b) Cory, R. M.; McPhail, C. L.; Dikmans, A. J.; Vittal, J. J. *Tetrahedron Lett.* **1996**, *37*, 1983. (c) Neudorff, W. D.; Lentz, D.; Anibarro, M.; Schlüter, A. D. *Chem. - Eur. J.* **2003**, *9*, 2745. (d) Stuparu, M.; Gramlich, V.; Stanger, A.; Schlüter, A. D. *J. Org. Chem.* **2007**, *72*, 424. (e) Stuparu, M.; Lentz, D.; Rüegger, H.; Schlüter, A. D. *Eur. J. Org. Chem.* **2007**, *2007*, 88. (f) Denekamp, C.; Etinger, A.; Amrein, W.; Stanger, A.; Stuparu, M.; Schlüter, A. D. *Chem. - Eur. J.* **2008**, *14*, 1628. (g) Lyoda, M.; Kuwatani, Y.; Yamauchi, T.; Oda, M. *J. Chem. Soc., Chem. Commun.* **1988**, 65. (h) Diercks, R.; Vollhardt, K. P. C. *J. Am. Chem. Soc.* **1986**, *108*, 3150. (i) Mohler, D. L.; Vollhardt, K. P. C.; Wolff, S. *Angew. Chem., Int. Ed. Engl.* **1990**, *29*, 1151.

(7) Scholl, R.; Meyer, K. *Ber. Dtsch. Chem. Ges. B* **1932**, *65*, 902.

(8) (a) King, B. T.; Kroulik, J.; Robertson, C. R.; Rempala, P.; Hilton, C. L.; Korinek, J. D.; Gortari, L. M. *J. Org. Chem.* **2006**, *71*, 5067. (b) Zhai, L.; Shukla, R.; Rathore, R. *Org. Lett.* **2009**, *11*, 3474. (c) Dössel, L.; Gherghel, L.; Feng, X.; Müllen, K. *Angew. Chem., Int. Ed.* **2011**, *50*, 2540. (d) Arslan, H.; Uribe-Romo, F. J.; Smith, B. J.; Dichtel, W. R. *Chem. Sci.* **2013**, *4*, 3973.

(9) (a) Nishiuchi, T.; Feng, X.; Enkelmann, V.; Wagner, M.; Müllen, K. *Chem. - Eur. J.* **2012**, *18*, 16621. (b) Golling, F. E.; Quernheim, M.; Wagner, M.; Nishiuchi, T.; Müllen, K. *Angew. Chem., Int. Ed.* **2014**, *53*, 1525. (c) Quernheim, M.; Golling, F. E.; Zhang, W.; Wagner, M.; Räder, H.-J.; Nishiuchi, T.; Müllen, K. *Angew. Chem., Int. Ed.* **2015**, *54*, 10341.

(10) Sisto, T. J.; Zakharov, L. N.; White, B. M.; Jasti, R. *Chem. Sci.* **2016**, Advance Article. DOI: 10.1039/C5SC04218F.

(11) (a) Nakamura, E.; Tahara, K.; Matsuo, Y.; Sawamura, M. *J. Am. Chem. Soc.* **2003**, *125*, 2834. (b) Matsuo, Y.; Tahara, K.; Sawamura, M.; Nakamura, E. *J. Am. Chem. Soc.* **2004**, *126*, 8725.

DOI: 10.1021/jacs.6b02240
J. Am. Chem. Soc. 2016, 138, 6577−6582

(12) (a) Omachi, H.; Segawa, Y.; Itami, K. *Acc. Chem. Res.* **2012**, *45*, 1378. (b) Yamago, S.; Kayahara, E.; Iwamoto, T. *Chem. Rec.* **2014**, *14*, 84. (c) Lewis, S. E. *Chem. Soc. Rev.* **2015**, *44*, 2221.
(13) (a) Jasti, R.; Bhattacharjee, J.; Neaton, J. B.; Bertozzi, C. R. *J. Am. Chem. Soc.* **2008**, *130*, 17646. (b) Sisto, T. J.; Golder, M. R.; Hirst, E. S.; Jasti, R. *J. Am. Chem. Soc.* **2011**, *133*, 15800. (c) Hirst, E. S.; Jasti, R. *J. Org. Chem.* **2012**, *77*, 10473. (d) Golder, M. R.; Jasti, R. *Acc. Chem. Res.* **2015**, *48*, 557. (e) Darzi, E. R.; Sisto, T. J.; Jasti, R. *J. Org. Chem.* **2012**, *77*, 6624. (f) Xia, J.; Jasti, R. *Angew. Chem., Int. Ed.* **2012**, *51*, 2474.
(14) Bonifacio, M. C.; Robertson, C. R.; Jung, J.-Y.; King, B. T. *J. Org. Chem.* **2005**, *70*, 8522.
(15) Sakurai, H.; Daiko, T.; Hirao, T. *Science* **2003**, *301*, 1878.
(16) Kumar, B.; Viboh, R. L.; Bonifacio, M. C.; Thompson, W. B.; Buttrick, J. C.; Westlake, B. C.; Kim, M.-S.; Zoellner, R. W.; Varganov, S. A.; Mörschel, P.; Teteruk, J.; Schmidt, M. U.; King, B. T. *Angew. Chem., Int. Ed.* **2012**, *51*, 12795.
(17) Collins, S. K.; Grandbois, A.; Vachon, M. P.; Côté, J. *Angew. Chem., Int. Ed.* **2006**, *45*, 2923.
(18) Martin, R.; Buchwald, S. L. *Acc. Chem. Res.* **2008**, *41*, 1461.
(19) (a) Barder, T. E.; Walker, S. D.; Martinelli, J. R.; Buchwald, S. L. *J. Am. Chem. Soc.* **2005**, *127*, 4685. (b) Kinzel, T.; Zhang, Y.; Buchwald, S. L. *J. Am. Chem. Soc.* **2010**, *132*, 14073.
(20) Clar, E.; John, F.; Avenarius, R. *Ber. Dtsch. Chem. Ges. B* **1939**, *72*, 2139.
(21) (a) Hitosugi, S.; Nakanishi, W.; Yamasaki, T.; Isobe, H. *Nat. Commun.* **2011**, *2*, 492. (b) Hitosugi, S.; Yamasaki, T.; Isobe, H. *J. Am. Chem. Soc.* **2012**, *134*, 12442. (c) Sato, S.; Yamasaki, T.; Isobe, H. *Proc. Natl. Acad. Sci. U. S. A.* **2014**, *111*, 8374. (d) Sun, Z.; Sarkar, P.; Suenaga, T.; Sato, S.; Isobe, H. *Angew. Chem., Int. Ed.* **2015**, *54*, 12800. (e) Yagi, A.; Segawa, Y.; Itami, K. *J. Am. Chem. Soc.* **2012**, *134*, 2962. (f) Iwamoto, T.; Kayahara, E.; Yasuda, N.; Suzuki, T.; Yamago, S. *Angew. Chem., Int. Ed.* **2014**, *53*, 6430. (g) Matsuno, T.; Sato, S.; Iizuka, R.; Isobe, H. *Chem. Sci.* **2015**, *6*, 909.
(22) For other impressive fully conjugated macrocycles containing large PAHs, see Müllen's work in ref 9.
(23) (a) Kayahara, E.; Patel, V. K.; Yamago, S. *J. Am. Chem. Soc.* **2014**, *136*, 2284. (b) Patel, V. K.; Kayahara, E.; Yamago, S. *Chem. - Eur. J.* **2015**, *21*, 5742.
(24) Kubota, N.; Segawa, Y.; Itami, K. *J. Am. Chem. Soc.* **2015**, *137*, 1356.
(25) CCDC 1421390 (**1**) and 1421391 (**2**) contain the supplementary information crystallographic data for this paper. These data can be obtained free of charge from The Cambridge Crystallographic Data Centre via www.ccdc.cam.ac.uk/data_request/cif.
(26) Segawa, Y.; Šenel, P.; Matsuura, S.; Omachi, H.; Itami, K. *Chem. Lett.* **2011**, *40*, 423.
(27) (a) Bodwell, G. J.; Fleming, J. J.; Miller, D. O. *Tetrahedron* **2001**, *57*, 3577. (b) Ghasemabadi, P. G.; Yao, T.; Bodwell, G. J. *Chem. Soc. Rev.* **2015**, *44*, 6494.
(28) (a) Merner, B. L.; Dawe, L. N.; Bodwell, G. J. *Angew. Chem., Int. Ed.* **2009**, *48*, 5487. (b) Merner, B. L.; Unikela, K. S.; Dawe, L. N.; Thompson, D. W.; Bodwell, G. J. *Chem. Commun.* **2013**, *49*, 5930.
(29) For full optical and electrochemical characterization of **1**, **2**, and **3**, see Figures S3−S13 in the Supporting Information.
(30) (a) Fujitsuka, M.; Cho, D.; Iwamoto, T.; Yamago, S.; Majima, T. *Phys. Chem. Chem. Phys.* **2012**, *14*, 14585. (b) Darzi, E. R.; Jasti, R. *Chem. Soc. Rev.* **2015**, *44*, 6401.
(31) (a) Li, P.; Sisto, T. J.; Darzi, E. R.; Jasti, R. *Org. Lett.* **2014**, *16*, 182. (b) Segawa, Y.; Fukazawa, A.; Matsuura, S.; Omachi, H.; Yamaguchi, S.; Irle, S.; Itami, K. *Org. Biomol. Chem.* **2012**, *10*, 5979. (c) Wong, B. M. *J. Phys. Chem. C* **2009**, *113*, 21921. (d) Iwamoto, T.; Watanabe, Y.; Sakamoto, Y.; Suzuki, T.; Yamago, S. *J. Am. Chem. Soc.* **2011**, *133*, 8354−8361.
(32) Anodic potentials (reductions) are presented in Figures S10, S12, and S13 in the Supporting Information.
(33) See the Supporting Information for the full citation: Frisch, M. J.; et al., *Gaussian 09*, revision B.01; Wallingford, CT, 2009.
(34) Segawa, Y.; Omachi, H.; Itami, K. *Org. Lett.* **2010**, *12*, 2262.

DOI: 10.1021/jacs.6b02240
J. Am. Chem. Soc. 2016, 138, 6577−6582